Mitigation of Static Carrier Phase Multipath Effects Using Multiple Closely-Spaced Antennas

JAYANTA K. RAY and M. ELIZABETH CANNON

Department of Geomatics Engineering, University of Calgary, Calgary, Canada

Telephone: (403) 220 3593 Fax: (403) 284 1980

PATRICK C. FENTON

Novatel Inc., Calgary, Canada

ABSTRACT

The effect of carrier phase multipath in static mode is investigated and a system is developed to reduce the effect using multiple closely-spaced antennas. The correlated nature of multipath, along with the known geometry among the antennas are used to estimate and mitigate carrier phase multipath. The mathematical model of the multipath effects on carrier phase measurements and the Kalman filter implemented to estimate these errors are described. The model is first tested on simulated data and later on field data collected on a roof whereby the model adaptively estimates the parameters of the composite multipath signal. Initial results shows that, the RMS value of the average multipath error on a single differenced carrier phase measurement data is typically reduced by over 70% percent.

INTRODUCTION

The influence of multipath signals on carrier phase measurements is one of the limitations to achieving high accuracy positions in a wide variety of applications. The problem is especially a concern for GPS reference stations whereby the static environment may induce slowly changing specular effects which do not easily average out.

Significant work has been done to characterize the effects of multipath on a Delay Lock Loop (DLL) in a PRN receiver [1], [2], [3] and to reduce these effects using various methods which can be broadly classified as

- Antenna-based mitigation
- Improved receiver technology
- Signal and data processing

Antenna based mitigation involves improving the antenna gain pattern to counter the multipath. A choke ring with a ground plane has been very effective in this regard. By designing an antenna with a very low gain for left hand circularly polarized (LHCP) signals and using an antenna array to have a sharp cutoff below a certain elevation angle, significant improvements can be achieved [4]. Various methods to mitigate code multipath by using a Multiple Signal Classification (MUSIC) technique with multiple antennas and an extended Multipath Estimation Delay Lock Loop (MEDLL) are described in [5].

A comprehensive overview of receiver technologies to mitigate multipath is given in [6]. Some of the special techniques are Narrow Correlator Spacing [7], [8], the Multipath Elimination Technique [9], MEDLL [10] and the Strobe Correlator Technique [11].

Multipath mitigation using the signal-to-noise ratio is explored in [12], while [13] investigate the use of multiple reference stations. Carrier phase smoothing is another way to reduce multipath on pseudorange measurements [14].

The effect of multipath on the carrier phase is characterized in [3]. Overall, however there is less literature on mitigation strategies [15]. One technique, given in [16] uses L1-L2 measurements to estimate the carrier phase multipath error using the relationship between the frequency of the carrier phase multipath error and the carrier wavelength. Tests showed however, that the performance was not satisfactory due to unmodeled phase center variation and antenna imaging resulting from the attached aluminum box used in the experiment. Another technique called the Enhanced Strobe Correlator, rejects carrier phase multipath, but in a strong and fast-changing multipath environment, it does not completely eliminate the effect [11].

These limitations highlight the need for alternative approaches for carrier phase multipath mitigation and thus provides the motivation for this research.

EFFECT OF MULTIPATH ON CARRIER PHASE

A GPS receiver generally receives a number of reflected signals along with the direct signal from the satellite. These reflected signals are called multipath signals and impact the input satellite signal to a GPS receiver. The composite input signal can be expressed as,

$$s(t) = d(t)c(t)A\sum_{i=0}^{n}\alpha_i \cos(2\pi f_L t + \theta_0 + \frac{2\pi d_i}{\lambda}) \qquad (1)$$

where,

- d(t) is the navigation data bit
- c(t) is the GPS C/A code
- A is the carrier signal amplitude
- α_i are the direct and reflected signal coefficient
- f_L is the GPS carrier frequency (Hz)
- d_i is the signal path delay with respect to direct signal (m)
- λ is the GPS signal wavelength (m)
- θ_0 is the initial phase, (rad) and
- n is the number of reflected signals.

Here, d_i and α_i vary with time. Also for the direct signal (i.e. i=0), $d_0 = 0$ and $\alpha_0 = 1$.

In the receiver, the incoming signal is beat with the local carrier in Inphase and Quadraturephase loops after (or sometimes before) the DLL. Neglecting the effect of the navigation data bits, the discriminator output is,

$$\Psi = \arctan\left(\frac{\sum_{i=0}^{n} R(\tau - d_i)\alpha_i \sin\left(\psi + \frac{2\pi d_i}{\lambda}\right)}{\sum_{i=0}^{n} R(\tau - d_i)\alpha_i \cos\left(\psi + \frac{2\pi d_i}{\lambda}\right)}\right) \qquad (2)$$

where,

$R(\tau)$ is the correlation function

Ψ is the measured carrier phase (rad), and

ψ is the true carrier phase (rad).

In the absence of reflected signals, $\alpha_0 = 1$, $\alpha_1 \ldots . \alpha_n = 0$, and $d_0 = 0$, so the equation reduces to $\Psi = \psi$; i.e. the measured phase is the same as the true phase. In the presence of reflected signals, the carrier phase measurement error due to multipath is $\Delta\Psi = \Psi - \psi$.

It is possible to assume a virtual reflector with time varying parameters (reflection co-efficient and location) as a representation of all the reflectors in the vicinity of the antenna. The effect of all the reflected signals can then be assumed to be due to this single virtual reflector.

The variability of the reflection parameters of the virtual reflector can be expressed as a function of time. Then multipath error due to a single reflector can be derived from Equation 2 and is given by [3] as

$$\Delta\Psi = \arctan\left(\frac{R(\tau-\delta(t))\alpha(t)\sin\gamma(t)}{R(\tau)+R(\tau-\delta(t))\alpha(t)\cos\gamma(t)}\right) \qquad (3)$$

where, $\gamma(t)$ is the multipath relative phase.

By dividing the numerator and denominator of equation (3) by $R(\tau)$ and describing $\alpha(t)R(\tau - \delta(t))/R(\tau)$ as $\alpha_1(t)$, the following form results,

$$\Delta\Psi = \arctan\left(\frac{\alpha_1(t)\sin\gamma(t)}{1+\alpha_1(t)\cos\gamma(t)}\right) \qquad (4)$$

which is the relationship between the carrier phase error due to multipath and the reflected signal strength and relative phase.

In a situation where multiple antennas are placed nearby, reflected signals on each of the antennas will be highly correlated. The difference in carrier phase error at two closely-spaced antennas due to multipath, assuming the reflection coefficient to be the same for both antennas, is then given by,

$$\Delta\Psi_0 - \Delta\Psi_1 = \arctan\left(\frac{\begin{array}{l}\alpha_1(t)\sin\gamma_0(t) - \alpha_1(t)\sin\gamma_1(t) \\ +\alpha_1^2(t)\sin(\gamma_0(t) - \gamma_1(t))\end{array}}{\begin{array}{l}1 + \alpha_1(t)\cos\gamma_0(t) - \alpha_1(t)\cos\gamma_1(t) \\ +\alpha_1^2(t)\cos(\gamma_0(t) - \gamma_1(t))\end{array}}\right) \quad (5)$$

where the subscripts 0 and 1 refer to Antennas 0 and 1. This model is used to develop the multipath mitigation filter described below, since it relates the measurement data and the state parameters to be estimated.

MULTIPATH MITIGATION MODEL

The multipath mitigation algorithm is a software suite which processes raw carrier phase measurement data from an antenna array before the data is used for kinematic position determination. Although this technique can be used to correct phase measurements in real-time, it is implemented in post mission in the sequel.

In the mitigation algorithm, the virtual reflector represents the total sum of all the associated reflectors and is modeled as a single reflector. For this reason it is appropriate to analyze the concept using the single reflector case.

The reflection of a satellite signal can be viewed from a geometrical perspective. For example, if the satellite is far away, the GPS signal can be assumed to arrive as parallel rays at two closely-spaced antennas. A plane wavefront, perpendicular to the line of sight, can be assumed to have the same carrier phase. After reflection from a plane reflector, the parallel incident signals remain parallel and thus phase propagation takes place through the advancement of the plane wavefront. Therefore, the phase of the reflected signal at each antenna phase center in a group of closely-spaced antennas is a function of the reflected signal direction (i.e. azimuth and elevation) as well as the relative geometry of the antennas with respect to each other.

In Figure 1 two antennas are placed at Antennas 0 and 1. Each of the antennas receives a direct signal from the satellite and a reflected signal from a nearby plane object. A wavefront perpendicular to the

indirect signal at Antenna 0 will have the same phase for all the other parallel reflected rays from the same object. Therefore, assuming that both Antennas 0 and 1 are on the same local horizontal plane, the phase of the reflected signal at Antenna 1 is given by,

$$\gamma_1 = \gamma_0 + \frac{2\pi}{\lambda} a_{01} \cos(\varphi_0 - \phi_{01}) \cos\theta_0 \qquad (6)$$

where,

γ_0 is the phase of the signal at Antenna 0 (rad)

a_{01} is the distance between 0 and 1 (m)

φ_0 is the azimuth of the reflected signal (rad)

ϕ_{01} is the azimuth of the vector 0-1 (rad), and

θ_0 is the elevation of the reflected signal (rad).

FIGURE 1

If the phase and direction of the reflected signal at Antenna 0 are known, the phase at Antenna 1 can be computed from the known geometry between the two antennas. This relationship is exploited to estimate the reflected signal phase at each of the antennas in the array, thereby reducing the number of unknowns in the system.

The parameters of the reflected signal are estimated using an Extended Kalman Filter [18], [19], [20]. Multiple antennas are placed close together to ensure correlated multipath signals. As described in the later section, single difference carrier phases between antennas are used as measurements for the Kalman filter and therefore to estimate four unknown parameters at least five antennas would be required. A typical layout would be (for the six antenna case) as shown in Figure 2.

FIGURE 2

One of the antennas (normally the center one) would be defined as the reference antenna (A0 in this case). All the parameters of the reflected signal and the placement of other antennas are defined with respect to this reference antenna.

The state vector for the estimator is,

$$\begin{bmatrix} \alpha \\ \gamma_0 \\ \theta_0 \\ \varphi_0 \end{bmatrix} = \begin{bmatrix} \text{Reflection coefficient} \\ \text{Reflected signal phase at the reference antenna} \\ \text{Reflected signal elevation} \\ \text{Reflected signal azimuth} \end{bmatrix}.$$

The measurement vector for the estimator is

$$\begin{bmatrix} \Delta\Psi_{0,1} \\ : \\ : \\ \Delta\Psi_{0,m-1} \end{bmatrix}$$

where,

m is the number of antennas, and

$\Delta\Psi_{0,1}$ is the difference in phase between Antennas 0 and 1.

The relationship between the state variables and the measurements is given by the following design matrix:

$$H = \begin{bmatrix} \frac{\delta(\Delta\Psi_{0,1})}{\delta\alpha} & \frac{\delta(\Delta\Psi_{0,1})}{\delta\gamma_0} & \frac{\delta(\Delta\Psi_{0,1})}{\delta\theta_0} & \frac{\delta(\Delta\Psi_{0,1})}{\delta\varphi_0} \\ --- & --- & --- & --- \\ --- & --- & --- & --- \\ \frac{\delta(\Delta\Psi_{0,m-1})}{\delta\alpha} & \frac{\delta(\Delta\Psi_{0,m-1})}{\delta\gamma_0} & \frac{\delta(\Delta\Psi_{0,m-1})}{\delta\theta_0} & \frac{\delta(\Delta\Psi_{0,m-1})}{\delta\varphi_0} \end{bmatrix} \quad (7)$$

Each element in the design matrix is obtained by substituting Equation 6 into Equation 5 and then computing the partial derivative with respect to the unknown parameters.

In the Kalman filter, the state variables are described as simple first order Gauss-Markov processes. The correlation time was selected to be around 1 minute and an appropriate process noise was chosen for each of the state variables. The selection of the process noise plays a crucial role in the estimation, as the filter is quite sensitive to this value.

The above filter is used to estimate the reflection parameter of a virtual reflector affecting the carrier phase measurement of a particular GPS satellite signal. One such filter per satellite is required to correct the carrier phase from each of the satellite signals in the receiver.

After the filter estimates the reflected signal phase at the reference antenna, it is possible to compute the phase at all the other antennas by using the relationship given in Equation (6). The reflected signal strength at all the antennas are assumed to be the same and is also estimated. After all the above mentioned parameters are estimated, the carrier phase error due to the composite multipath signal can be computed using Equation (5).

By using the above model, it is possible to estimate the carrier phase error due to multipath signals. This method is valid only if the reflected signals are correlated across the antennas, which is likely to happen if the antenna spacing is much smaller compared to the size of the reflector. Hence the need for closely-spaced antennas on a rigid platform.

TEST DESCRIPTION

A Multipath Simulation and Mitigation software program (MultiSiM) was first developed to study the behavior of simulated multipath signals and their mitigation. The multipath simulation module of MultiSiM allows the simulation of various multipath environments by placing reflectors and antennas at a desired geometry with respect to each other. In the multipath mitigation module of MultiSiM, different experimental multipath-countering models were incorporated to study their effectiveness in estimating the multipath effect. After having successfully demonstrated the mitigation of multipath using the above model on simulated multipath; the same approach was applied to real data as described below.

In order to test the concept, a special antenna array was assembled whereby a thick aluminum plate was used to rigidly mount six antennas close together. Novatel Model 521 antennas were used, as they are small with a diameter of approximately 5.6 cm. The assembly is shown in Figure 3.

FIGURE 3

NovAtel BeeLine™ receivers [21] were used for data collection. The BeeLine™ is an 8+8 channel (L1-L1) receiver generally used for the attitude determination. Three BeeLines™ were used together with six antennas where all receivers were driven by an external rubidium oscillator. Data was collected for several sessions spread over successive days on the roof of the Engineering building at the University of Calgary.

The antenna assembly was placed on a surveyed pillar where there are concrete sidewalls of approximately 3 m in height on the east side and 1 meter in height on the south side (Figure 4). It is expected that these walls, along with the aluminum plate, would cause the most significant multipath signals.

FIGURE 4

By using Semikin™ [22], a software package developed at the University of Calgary, the position of each of the antennas in the array was determined and their relative geometry established.

The modified carrier phase of single differences between antennas are used as measurements in the estimator. The single difference removes most of the errors except receiver clock bias, multipath and carrier phase noise. For example,

$$\Delta\Psi_{0,i} = \Delta\rho_{0,i} + \Delta N_{0,i}\lambda + c\Delta t_{0,i} + \varepsilon_{\varphi 0,i} + \varepsilon_{MP0,i} \qquad (8)$$

where,

- $\Delta\Psi$ is the measured carrier phase single difference between antennas 0 and i (m)
- $\Delta\rho$ is the range difference due to spatial separation between antennas
- $c\Delta t$ is the receiver clock bias difference
- ΔN is the integer ambiguity difference
- ε_{φ} is the carrier phase noise difference, and
- ε_{MP} is the carrier phase multipath error difference.

In the present case, since the receivers are driven by a single external stable clock, the receiver clock bias difference is negligible. In addition, since the phase difference due to the spatial separation of the antennas is known, the range difference then can be eliminated from equation (8) to give,

$$\Delta\Psi'_{0,i} = \Delta N_{0,i}\lambda + \varepsilon_{\varphi 0,i} + \varepsilon_{MP0,i} \qquad (9)$$

As the multipath induced error is less than a quarter of a cycle, the phase difference due to the relative integer ambiguity can be removed and the residual phase error can be obtained. This residual phase is due to the receiver carrier phase noise and the multipath between the receivers.

The single differenced residual carrier phase error for a particular satellite is input to the multipath mitigating software to adaptively estimate the parameters of the composite multipath signal due to all reflectors affecting the carrier phase. After the parameters are estimated by the filter, it is possible to determine the multipath error in the carrier phase at each of the antennas by using equations (5) and (6). The estimated multipath error at each antenna can be differenced and then subtracted from the single differenced phase residual (which was input) to observe a multipath-reduced phase measurement. The signature of the residual phase difference with the multipath error correction (which should be white due to receiver phase noise) can be analyzed to assess the performance of the technique.

TEST RESULTS

The single differenced residual described in the previous section contains the carrier phase noise and multipath error. Carrier phase noise is random in nature, while the multipath error is oscillatory where the amplitude depends upon the material and surface structure of the reflector as well as the distance between the reflector and antenna. The frequency of the multipath error is a function of the carrier cycle wavelength and the antenna reflector geometry (Georgiadou and Kleusberg, 1988).

In order to demonstrate the multipath mitigation technique, the single differenced residual phase was computed for satellite 21 from data collected on August 25, 1998 and is shown in Figure 5. Each plot has a distinct trend, which is different for each antenna. Some oscillatory errors of varying amplitude are also

evident. Data collected on the subsequent two days (at 4 minutes earlier than the previous day) also show a similar trend and oscillation pattern. The residual phase for the same satellite from the data collected on August 26 is shown in Figure 6.

Here, the level of multipath seems to be quite high, possibly due to the deliberate unfavorable environment at which the system was tested. The day-to-day repeatability of the residual errors indicates that it is due to multipath. An average correlation of 85% was observed between data collected on August 25 and 26.

FIGURE 5

FIGURE 6

The multipath error consists of two distinct components in this case, i.e. the slow trend is due to multipath from a nearby strong reflector while the smaller oscillatory errors (or higher frequency multipath) are due to weaker reflectors from objects further away. The non-uniformity of the oscillatory pattern suggests multiple reflectors in the vicinity of the antenna assembly. All other satellites show similar trends and oscillatory patterns, which repeat day-to-day.

In Figures 5 and 6 it can also be observed that the higher frequency multipath error is correlated among the antennas. In contrast, the lower frequency multipath has a different trend for different antennas. This is because the lower frequency multipath changes its phase very slowly and has a different phase at each antenna depending upon the antenna reflector geometry. Another possible explanation of the low frequency trends in the residuals is that the position of the antennas in the antenna assembly were not computed accurately enough due to antenna gain pattern interference and high multipath in the carrier phase measurements. In any case, such a high correlation of multipath across antennas is due to the close antenna spacing in the assembly and is critical to the estimation of composite reflected signal parameters using the algorithms described in the previous sections.

The multipath-corrupted carrier phase measurement residuals are used as input to the mitigating filter. Figure 7 shows the parameters of the composite reflected signal estimated by the filter for SV 21 on

August 25. The parameters of the virtual reflector vary with time to track the effect of the composite multipath error.

FIGURE 7

Figure 8 shows the estimated multipath error at each antenna computed from the estimated parameters of the composite reflected signal. The estimated multipath shows a trend and oscillations corresponding to low and high frequency multipath, respectively, and this demonstrates the capability of the system to estimate a composite reflection effect, rather than a single reflector.

FIGURE 8

The carrier phase measurement from each antenna can be corrected by the estimated multipath error at that antenna. Figure 9 shows the single differenced residual with the corrected measurement data. It is clear from the figure that the residuals are more random in nature and that phase error due to multipath is nearly eliminated.

FIGURE 9

FIGURE 10

Figure 10 shows the multipath corrected measurement data for the same satellite on August 26. As in the previous case, the multipath correction is nearly eliminated except during the filter convergence period.

FIGURE 11

FIGURE 12

Figures 11 and 12 show the single differenced residual before and after applying the multipath mitigation technique for satellite 31 on August 25. These results are in agreement with SV 21.

This method was applied to other satellites available during the data collection period and the improvement of residuals is observed in all cases. Table 1 gives an overview of statistics before and after

multipath mitigation. These statistics were compiled from approximately 4000 samples excluding the convergence period and were averaged over all the antennas.

TABLE 1

The RMS values of the multipath-corrected measured phase differences are significantly lower than the values before correction. On average, there was a 73% improvement, which clearly demonstrates the effectiveness of this method to mitigate carrier phase multipath in this environment.

CONCLUSIONS AND FUTURE WORK

The effect of multipath on GPS carrier phase measurement data is investigated using field data. Tests were carried out on the roof of the Engineering building at the University of Calgary. Six closely-spaced antennas and three Novatel BeeLine^{TM} receivers were used for the experiment and the carrier phase multipath signature was found to be highly correlated across the antennas.

A method to estimate the total effect of multipath from all sources on GPS carrier phase data was developed and consists of a filter which estimates the reflection coefficient, multipath signal phase and direction using the single difference phase measurements between antennas as input. Initial results show that the proposed technique is capable of estimating the composite multipath effect on the carrier phase, which can be easily removed from the measurement. On average, 73% of the carrier phase multipath was removed in the test environment.

This technique estimates the parameters of the composite multipath signal and removes the error due to all multipath signals. It is particularly useful for reference stations which transmit carrier phase data for kinematic positioning applications.

Further investigations with a better ground plane and in different multipath environments are needed to further assess the performance of the system. The estimator also needs to be further tuned by choosing a more suitable system dynamic model and as well as process noise parameters for superior performance.

The applicability of the system to real time application will also be analyzed to exploit the potential of this system.

ACKNOWLEDGMENTS

Thanks to Waldemar Kunysz of NovAtel Inc. for technical support and logistics. One of the first authors (J.K.R) thanks Nesbitt Burns Inc. and Canadian Natural Resources Limited for their financial support during his graduate program.

Based on a paper presented at the ION GPS-98, Nashville, September 1998.

REFERENCES

1. Hagerman, L.L. (1973), *Effects of Multipath on Coherent and Non-coherent PRN Ranging Receiver*, Aerospace Report No. TOR-0073 (3020 – 03) –3, Development Planning Division, The Aerospace Corporation, 39 pp.
2. Breeuwer, E. (1992), *Modeling and Measuring GPS Multipath Effects*, Master's Thesis, Faculty of Electrical Engineering, Delft University of Technology, Delft, The Netherlands, January 1992. 117 pp.
3. Braasch, M.S. (1996), *Multipath Effects, Global Positioning Systems: Theory and Applications*, American Institute of Aeronautics and Astronautics, Vol. 1, Ch 14, pp. 547-568.
4. Bartone, C. and Frank van Graas (1998), *Airport Pseudolites for Local Area Augmentation*, Proceedings of IEEE PLANS, Catalogue No. 98CH36153, Palm Springs, April 20-23, pp. 479-486.
5. Moelker, D. (1997), *Multiple Antennas for Advanced GNSS Multipath Mitigation and Multipath Direction Finding*, Proceedings of ION GPS-97, September 16-19, Kansas City, pp. 541-550.
6. van Dierendonck, A.J. and M.S. Braasch (1997), *Evaluation of GNSS Receiver Correlation Processing Techniques for Multipath and Noise Mitigation,* Proceedings of the 1997 National Technical Meeting, Santa Monica, pp. 207-215.

7. Fenton, P., B. Falkenberg, T. Ford, K. Ng, A.J. van Dierendonck (1991), *Novatel's GPS Receiver: The High Performance OEM Sensor of the Future*, Proceedings of ION GPS-91, Albuquerque, September 9-13, pp. 49-58.
8. van Dierendonck, A.J., P. Fenton and T. Ford (1992), *Theory and Performance of Narrow Correlator Technology in GPS Receiver*, Navigation: Journal of The Institute of Navigation, Vol. 39, No. 3, pp. 265-283.
9. Townsend, B. and P. Fenton (1994), *A Practical Approach to the Reduction of Pseudorange Multipath Errors in a L1 GPS Receiver,* Proceedings of ION GPS-94, Salt Lake City, September 20-23, pp. 143-148.
10. van Nee, R.D.J (1994), *The Multipath Estimating Delay Lock Loop: Approaching Theoretical Accuracy Limits*, Proceedings of IEEE PLANS, Las Vegas, April 11-15, pp. 246-251.
11. Garin L and J. Rousseau (1997), *Enhanced Strobe Correlator Multipath Rejection for Code & Carrier*, Proceedings of ION GPS-97, September 16-19, Kansas City, pp. 559-568.
12. Axelrad, P., C. Comp, and P. MacDoran, (1994), *Use of Signal-To-Noise Ratio for Multipath Error Correction in GPS Differential Phase Measurements: Methodology and Experimental Results*, Proceedings of ION GPS-94, Salt Lake City, September 20-23, pp. 655-666.
13. Raquet, Capt. J and G. Lachapelle (1996), *Determination and Reduction of GPS Reference Station Multipath using Multiple Receivers*, Proceedings of ION GPS-96, September 17-20, Kansas City, pp. 673-681.
14. Hatch, R. (1982), *The Synergism of GPS Code and Carrier Measurement*, Proceedings of Third International Geodetic Symposium on Satellite Doppler Positioning, DMA/NGS, Washington, D.C., pp. 1213-1232.
15. Weill, L.R. (1997), *Conquering Multipath: The GPS Accuracy Battle, Innovation*, GPS World, Vol. 8, No. 4, April 1997, pp. 59-66.
16. Georgiadou, Y and A. Kleusberg (1988), *On Carrier Signal Multipath Effects in relative GPS Positioning*, manuscripta geodatica, Springer-Verlag, Vol. 13, No. 3, pp. 172-179.

17. Brown R.G. and P.Y.C. Hwang (1992), *Introduction to Radnom Signals and Applied Kalman Filtering*, second edition, John Wiley & Sons Inc., 502 pp.
18. Gelb, A. (1979), *Applied Optimal Estimation*, MIT Press, Massachusetts Institute of Technology, Massachusetts, Cambridge, 374 pp.
19. Maybeck, P.S. (1994), *Stochastic Models, Estimation, and Control*, Vol. 1, Navtech, Arlington, 423 pp.
20. Ford, T., W. Kunysz, R. Morris, J. Neumann, J. Rooney and T. Smit (1997), *Beeline RT20-a Compact, Medium Precision Positioning System with and Attitude*, Proceedings of ION GPS-97, Kansas City, pp. 687-695.
21. Cannon, M.E. (1993), *SEMIKIN™ Operating Manual*, Version 2.0, Department of Geomatics Engineering, The University of Calgary, Calgary, AB. Canada. 12 pp.

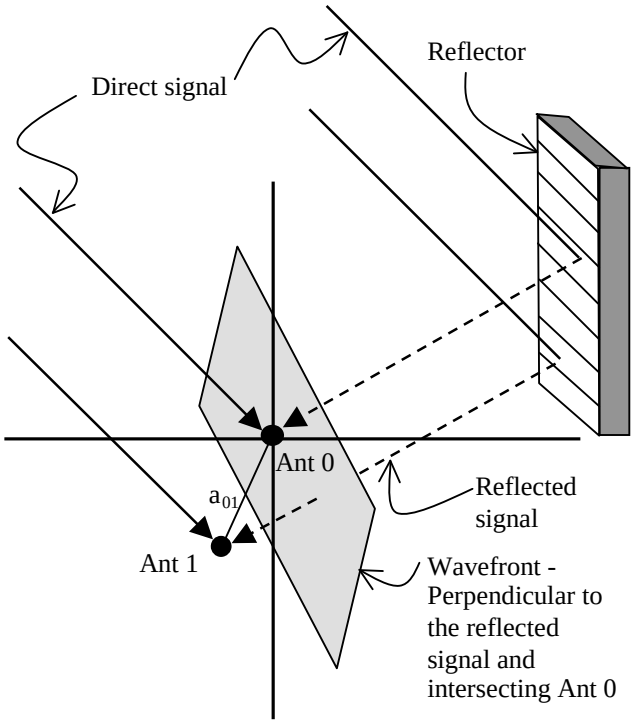

Figure 1: Correlated multipath errors can be related to each other through signal direction and known geometry between the antennas.

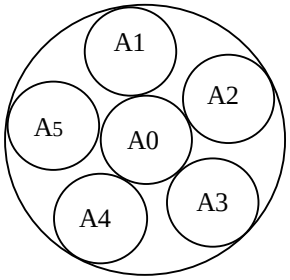

Figure 2: Typical antenna assembly for six antennas.

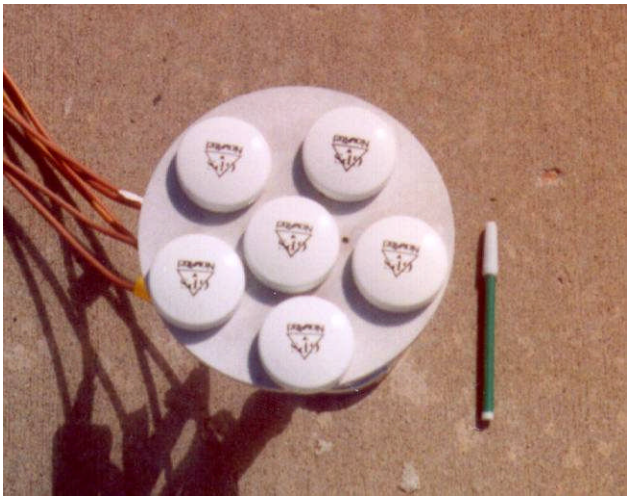

Figure 3: Antenna array assembly.

Figure 4: Test environment

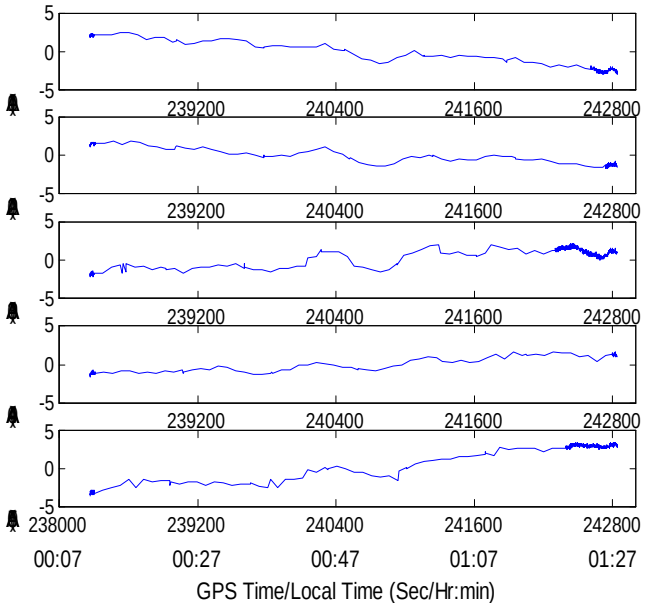

Figure 5: Single difference residual carrier phase error before applying multipath correction for SV 21 on August 25, 1998 (Y-axis units in cm; A0-An denotes single difference between antennas 0 and n).

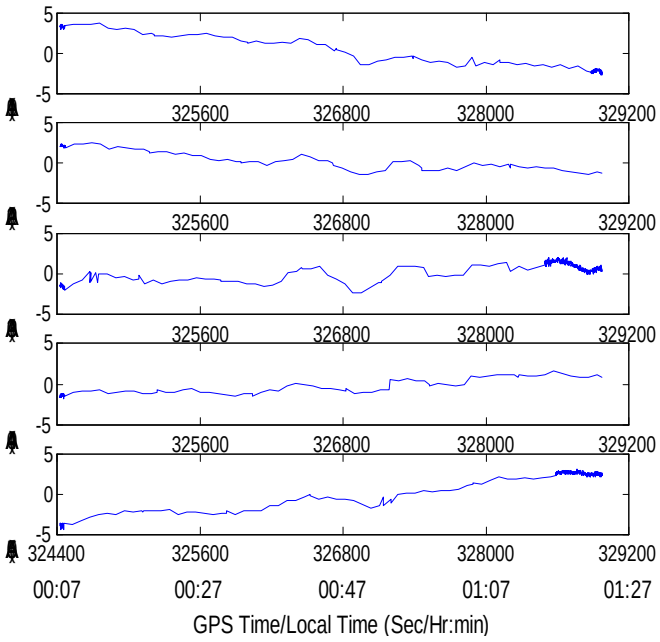

Figure 6: Single difference residual carrier phase error before applying multipath correction for SV 21 on August 26 for the same time of day (shifted by 4 minutes) as in Figure 5 (Y-axis in cm; A0-An denotes single difference between antennas 0 and n).

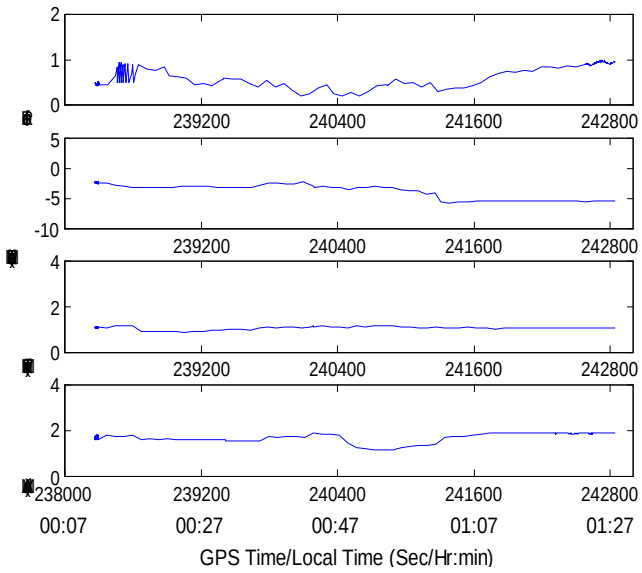

Figure 7: Estimated composite reflected signal parameters for SV 21 on August 25

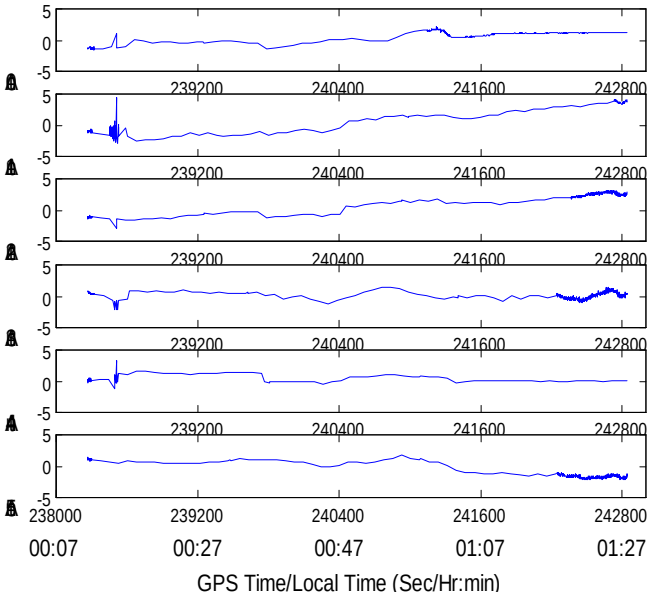

Figure 8: Estimated carrier phase multipath error for SV 21 on August 25 for each antenna (Y-axis in cm).

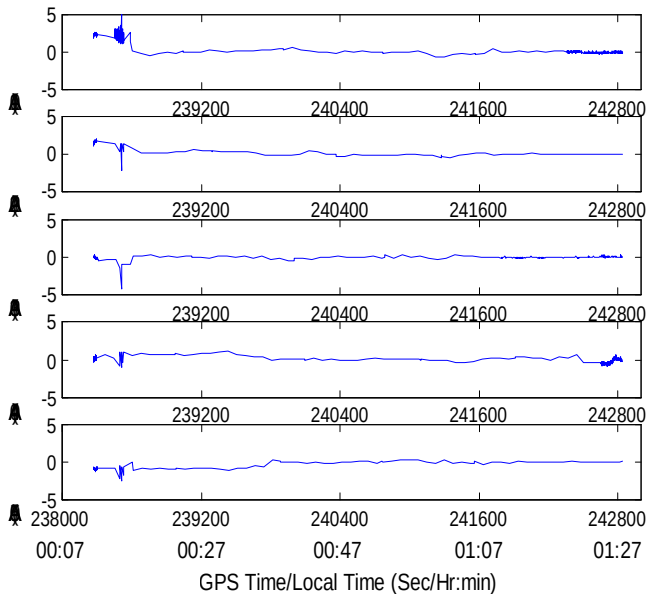

Figure 9: Single difference residual carrier phase error after removing estimated carrier phase multipath for SV 21 on August 25 (Y-axis in cm; A0-An denotes single difference between antennas 0 and n).

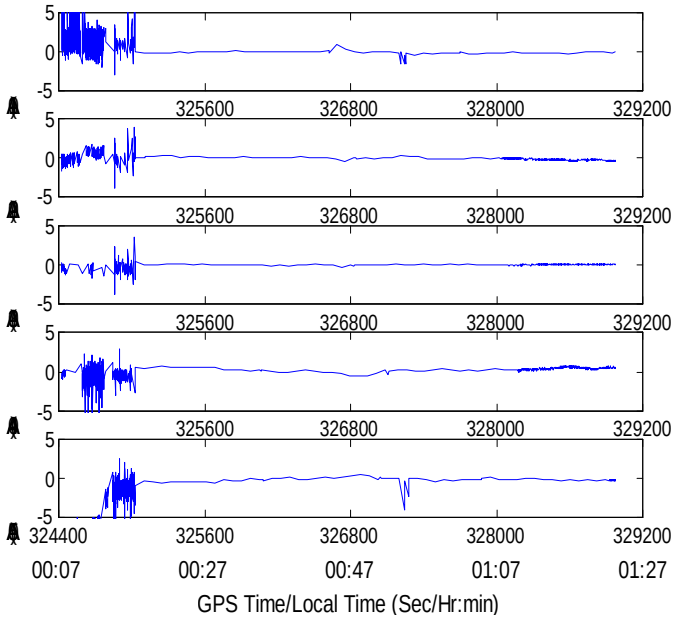

Figure 10: Single difference residual carrier phase error after removing estimated carrier phase multipath for SV 21 on August 26 (Y-axis in cm; A0-An denotes single difference between antennas 0 and n).

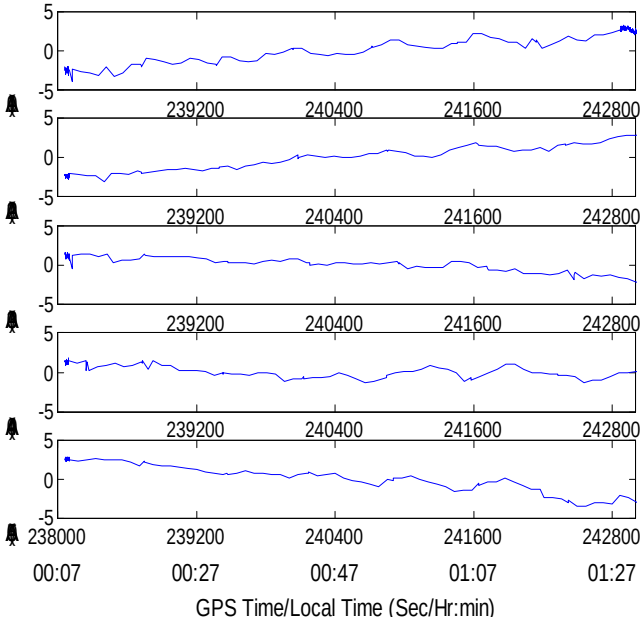

Figure 11: Single differenced residual carrier phase error before applying multipath correction for SV 31 on August 25 (Y-axis in cm; A0-An denotes single difference between antennas 0 and n).

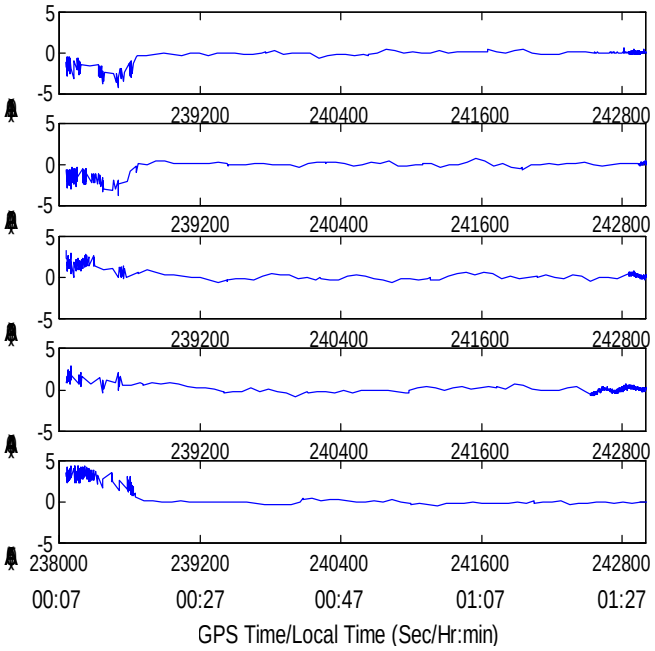

Figure 12: Single differenced residual carrier phase error after removing carrier phase multipath for SV 31 on August 25 (Y-axis in cm; ; A0-An denotes single difference between antennas 0 and n).

SV ID	August 25					August 26					Corr. coefficient before correction
	Before correction		After Correction		Impro-vement	Before correction		After correction		Impro-vement	
	Mean (cm)	RMS (cm)	Mean (cm)	RMS (cm)	%	Mean (cm)	RMS (cm)	Mean (cm)	RMS (cm)	%	
17	0.14	1.77	0.00	0.40	77.4	0.08	1.68	0.01	0.37	78.0	0.84
21	0.01	1.26	0.02	0.30	76.2	-0.08	1.28	-0.01	0.23	82.0	0.94
23	-0.19	1.70	0.26	0.59	65.3	-0.17	1.67	0.26	0.67	60.0	0.83
31	0.02	1.30	0.04	0.28	78.5	0.00	1.26	0.03	0.46	63.5	0.78

Table 1: Carrier phase error before and after applying the multipath mitigation technique.